Title

Modeling the potential contribution of land cover changes to the late twentieth century Sahel drought using a regional climate model: impact of lateral boundary conditions

Journal

Climate Dynamics, 47(11)

ISSN

0930-7575

Authors

Wang, Guiling
Yu, Miao
Xue, Yongkang

Publication Date

2016-12-01

DOI

10.1007/s00382-015-2812-x

Peer reviewed

Clim Dyn
DOI 10.1007/s00382-015-2812-x

Modeling the potential contribution of land cover changes to the late twentieth century Sahel drought using a regional climate model: impact of lateral boundary conditions

Guiling Wang[1] · Miao Yu[1,2] · Yongkang Xue[3]

Received: 16 March 2015 / Accepted: 22 August 2015

Abstract This paper investigates the potential impact of "idealized-but-realistic" land cover degradation on the late twentieth century Sahel drought using a regional climate model (RCM) driven with lateral boundary conditions (LBCs) from three different sources, including one re-analysis data and two global climate models (GCMs). The impact of land cover degradation is quantified based on a large number of control-and-experiment pairs of simulations, where the experiment features a degraded land cover relative to the control. Two different approaches of experimental design are tested: in the 1st approach, the RCM land cover degradation experiment shares the same LBCs as the corresponding RCM control, which can be derived from either reanalysis data or a GCM; with the 2nd approach, the LBCs for the RCM control are derived from a GCM control, and the LBCs for the RCM land cover degradation experiment are derived from a corresponding GCM land cover degradation experiment. When the 1st approach is used, results from the RCM driven with the three different sources of LBCs are generally consistent with each other, indicating robustness of the model response against LBCs; when the 2nd approach is used, the RCM results show strong sensitivity to the source of LBCs and the response in the RCM is dominated by the response of the driving GCMs. The spatiotemporal pattern of the precipitation response to land cover degradation as simulated by RCM using the 1st approach closely resembles that of the observed historical changes, while results from the GCMs and the RCM using the 2nd approach bear less similarity to observations. Compared with the 1st approach, the 2nd approach has the advantage of capturing the impact on large scale circulation, but has the disadvantage of being influenced by the GCMs' internal variability and any potential erroneous response of the driving GCMs to land degradation. The 2nd approach therefore requires a large ensemble to reduce the uncertainties derived from the driving GCMs. All RCM experiments based on the 1st approach produce a predominantly dry signal in West Africa throughout the year, with a dipole pattern found in the peak monsoon season that features a slight increase of precipitation over the Guinea Coast and strong decrease in the north; a similar spatiotemporal distribution is found for temperature changes, with warming (cooling) coinciding with precipitation decrease (increase). The model precipitation changes in West Africa are dominated by evapotranspiration changes in the north and by atmospheric moisture convergence changes in the south; in temperature changes, surface warming due to the decrease of evaporative cooling dominates over the albedo-induced radiative cooling.

This paper is a contribution to the special issue on West African Climate Decadal Variability and its modeling, consisting of papers from the West African Monsoon Modeling and Evaluation (WAMME) and the African Multidisciplinary Monsoon Analyses (AMMA) projects, and coordinated by Yongkang Xue, Serge Janicot, and William Lau.

✉ Guiling Wang
gwang@engr.uconn.edu

[1] Department of Civil and Environmental Engineering, Center for Environmental Sciences and Engineering, University of Connecticut, Storrs, CT, USA

[2] Collaborative Innovation Center on Forecast and Evaluation of Meteorological Disasters/Key Laboratory of Meteorological Disaster of Ministry of Education, Nanjing University of Information Science and Technology, Nanjing 210044, China

[3] Department of Geography, University of California, Los Angeles, CA, USA

Published online: 19 September 2015

Keywords Land use land cover changes · Sahelian drought · Dynamic downscaling · Regional climate modeling · Lateral boundary conditions · WAMME II

1 Introduction

Climate in West Africa has experienced significant variability at the intra-decadal and decadal time scales, characterized by a long persistent drought in the Sahel during the 2nd half of the twentieth century that caused enormous socioeconomic hardship. The region is especially vulnerable to precipitation fluctuations and potential climate changes due to its largely rain-fed agriculture. Despite potential future increase of precipitation in some portions of West Africa (e.g., Cook and Vizy 2012; Vizy et al. 2013; Yu et al. 2015), the warming and warming-induced drought are projected to cause decrease of crop yield over most of the region (Ahmed et al. 2015a). The climate-induced crop yield drop together with population increase necessitates expansion of agricultural land use (e.g., Ahmed et al. 2015b), which may further modify the regional climate. Reliable assessment of future climate change and its impact has to be based on solid understanding of past climate variability and how past land use land cover changes (LULCC) may have influenced the regional climate.

Land use and land cover in West Africa have gone through substantial changes in the past century in the form of degradation of vegetation cover and soil erosion, due primarily to overgrazing, fuelwood extraction, and agricultural expansion including cultivation of marginal land that was later abandoned. The potential impact of LULCC on West African climate has been a topic of active research since the 1970s, considered as a possible trigger or contributing factor for the late twentieth century Sahel drought. Research in this area has evolved from studies focused on a single parameter (e.g., Charney et al. 1977) to those using more complex land models that account for LULCC-induced changes in albedo, Bowen ratio, and surface roughness (e.g., Xue and Shukla 1993; Taylor et al. 2002; Hagos et al. 2014) as well as feedback due to vegetation dynamics (e.g., Zeng et al. 1999; Wang and Eltahir 2000a, b). While the regional and global sea surface temperature may have been an important trigger for the late twentieth century Sahel drought (e.g., Giannini et al. 2003; Lu and Delworth 2005; Hagos and Cook 2008), it is very likely that LULCC and vegetation processes acted as a contributing factor to the drought or an amplifier for the SST effects (e.g., Wang and Eltahir 2000a, Wang et al. 2004; Xue et al. 2010a, b; Kucharski et al. 2013).

Due to the lack of large scale observation before the satellite era, how and by how much the land cover in West Africa might have changed before and after the onset of the late twentieth century drought remain largely unknown, and are subjective to a high degree of uncertainty (Gornitz 1985; Fuller and Ottke 2002; Xue et al. 2004a). Most of the earlier studies on the climatic impact of LULCC were based on numerical experiments using coarse resolution global climate models (GCMs) or models of reduced complexity, and the magnitude and/or spatial extent of changes imposed on the land cover in the model were often unrealistically large. Recent studies have attempted to estimate the climatic impact of LULCC based on a more realistic magnitude of LULCC. Taylor et al. (2002) used a land use model to reconstruct past land cover changes in the Sahel region and applied these changes to a global climate model to examine its potential impact on precipitation in the region. They found a small magnitude of precipitation decrease that derives primarily from a delayed onset of the monsoon, but the magnitude of the precipitation decrease is not large enough to account for the observed drought. More recently, Hagos et al. (2014) applied a land cover change map from the second Experiment of the West African Monsoon Modeling and Evaluation, which is based on the historical land use data from Hurtt et al. (2011), and applied the changes to an ensemble of different configurations of the Weather and Research Forecast (WRF) model corresponding to different combinations of land surface and cumulus parameterization schemes. It was found that the response of the monsoon rainfall to the same prescribed land cover changes and the climatology of the model precipitation were both sensitive to the land surface scheme used, with weak response in relatively dry or relatively wet models and stronger response in models with smaller precipitation biases.

In addition to more realistic magnitude and extent of LULCC, it is also desirable that studies assessing the climate impact of LULCC make use of models with relatively fine spatial resolution to ensure regional relevance and to more realistically represent the spatial pattern/extent of LULCC (e.g., Abiodun et al. 2008; Paeth and Thamm 2007; Paeth et al. 2009; Hagos et al. 2014). This leads to the use of regional climate models (RCMs) due to the inhibiting expense of running GCMs at fine resolutions. Compared to GCMs, RCMs are better capable of capturing the spatial details of precipitation distribution in West Africa and in capturing the monsoon jump (a characteristic abrupt shift of the rain belt from around 5°N during the pre-monsoon season to 10°N at the monsoon onset) (e.g., Druyan et al. 2009; Xue et al. 2014). However, the use of RCMs brings a different set of challenges, due primarily to the need for lateral boundary conditions that have to be derived from reanalysis data or GCMs.

For any RCM, the use of a different set of LBCs influences not only the model precipitation climatology but also to some extent the climate change signal simulated by the

model (Yu and Wang 2014; Saini et al. 2015). As precipitation climatology may influence the response of a model climate to land surface forcing (LULCC or soil moisture changes) (Koster et al. 2004; Hagos et al. 2014), it is likely that the response of an RCM climate to LULCC may depend on the RCM LBCs. Moreover, when using an RCM to study the impact of surface condition changes such as LULCC or soil moisture changes within the RCM domain, different methodologies may be applied. One methodology uses the same LBCs for both the control and the experiment simulations (e.g., Abiodun et al. 2008; Paeth and Thamm 2007; Paeth et al. 2009; Hagos et al. 2014), which neglects the potential impact of surface condition changes on the LBCs and therefore implicitly assumes that the impact of surface conditions is constrained within the RCM domain. Alternatively, the RCM control and experiment can be driven with different LBCs that reflect the impact of surface condition changes on large scale circulation, which requires that a control simulation and an experiment be carried out using a GCM that applies the same surface condition changes as those in the RCM (e.g., Xue et al. 2012; Mei et al. 2013). It is not clear how these different methodologies may influence the RCM climate response to LULCC.

In this study, we examine the potential impact of "idealized-but-realistic" LULCC on climate in West Africa (especially the late twentieth century Sahel drought) using an RCM driven with LBCs from reanalysis data and from two GCMs. The questions of interest to this study include how the RCM results may depend on LBCs, how they may differ from the GCMs, how they differ between the two methodologies, and how they compare with observed changes associated with the late twentieth century Sahel drought. Section 2 describes the models and data used, and explains the details of experimental design. Section 3 documents the performance of the models in reproducing the spatial and temporal variability of precipitation in West Africa. Results are analyzed in Sect. 4, followed by discussion and conclusions in Sect. 5.

2 Models, data, and methodology

Three models are used in this study, including the Community Atmosphere Model version 5.0 (CAM5, Neale et al. 2012), the UCLA MRF GCM ("UCLA" hereafter, Kanamitsu et al. 2002; Xue et al. 2004b), and the regional climate model RegCM4.1 (Giorgi et al. 2012). The land surface model is SSiB-2 (Xue et al. 1991; Zhan et al. 2003) in UCLA and the Community Land Model version 4 (CLM4, Oleson et al. 2010) in CAM5. The default land surface model in RegCM4.1 was an earlier version of CLM (Steiner et al. 2009) but has been replaced with CLM4 in this study, and the resulting new model ("RegCM" hereafter) with additional modifications is described and its performance documented in Wang et al. (2015). Both CAM5 and UCLA are participating GCMs in WAMME2. In this study output from the CAM5 and UCLA WAMME2 control and land use change experiments are used to derive lateral boundary conditions (LBCs) for RegCM.

To evaluate the impact of LULCC on regional climate, paired model simulations are designed using CAM5, UCLA, and RegCM driven with different LBCs. Each pair includes a Control simulation and an LUC experiment that differ in their prescribed land cover. For both CAM5 and UCLA, each of the Control and LUC simulations was run for 6 years, with specified climatological SST based on the global Hadley SST for 1950–2009. The 6-hourly output from the last year of each GCM simulation is used as the driving LBCs for RegCM.

Three different sources of LBCs for RegCM are considered, including the National Centers for Environmental Prediction-Department of Energy (NCEP-DOE) AMIP-II reanalysis data (R2 hereafter) (Kanamistu et al. 2002), CAM5 output, and UCLA output. The corresponding RCM model simulations are hereafter referred to as RegCM(R2), RegCM(CAM5), and RegCM(UCLA). The RegCM(R2) Control and LUC simulations share the same LBCs, are run for 6 years over the period 2001–2006, and use the R2 sea surface temperature (SST) data for each corresponding year. Model outputs from the last 5 years of the simulations are used for analysis. All RegCM(CAM5) and RegCM(UCLA) simulations use climatological SST (which is the same as in the CAM5 and UCLA simulations) and cycle through the GCM-derived LBCs twice. Outputs from the last year of the simulations are used for analysis.

For each of the two RCM–GCM combinations [RegCM(CAM5) and RegCM(UCLA)], two different methodologies of land use experimental design are employed. In the first experiment (labelled as "LUC"), similar to the RegCM(R2) experiment, land cover change is incorporated into the model surface but the LBCs are the same as in the corresponding Control simulation. This methodology is referred to as the LUC approach in this study. In the second experiment (labelled as "LUC2"), in addition to land cover changes, the LBCs are derived from the corresponding GCM land cover change experiment. This methodology is referred to as the LUC2 approach in this study. Conceptually, the difference between the two is that LUC2 accounts for the impact of land-induced large scale circulation changes beyond the RegCM model domain on climate within the domain, while LUC does not.

Details of the experimental design are summarized in Table 1. All simulations using RegCM were conducted at a 50 km horizontal resolution with 18 levels in the vertical

Table 1 Experimental design

Model used and experiments name	RCM LBCs	Land cover	SST Forcing	Simulation length (years)
CAM5				
Control	N/A	Control	Climatology	6
LUC	N/A	LUC	Climatology	6
UCLA				
Control	N/A	Control	Climatology	6
LUC	N/A	LUC	Climatology	6
RegCM(R2)				
Control	R2	Control	2001–2006 SST	6
LUC	R2	LUC	2001–2006 SST	6
RegCM(CAM5)				
Control	CAM5 Control	Control	Climatology	2
LUC	CAM5 Control	LUC	Climatology	2
LUC2	CAM5 LUC	LUC	Climatology	2
RegCM(UCLA)				
Control	UCLA Control	Control	Climatology	2
LUC	UCLA Control	LUC	Climatology	2
LUC2	UCLA LUC	LUC	Climatology	2

direction, and the model domain covers the region approximately 33°W–55°E and 21°S–36°N. This places West Africa in the center of the domain, away from the adverse effects near the boundaries. A recent study by Sylla et al. (2015) found that increasing the model resolution from 50 to 25 km led to no major improvement of the model performance in this region. For the GCM simulations, CAM5 was run at the T63L26 resolution (close to a horizontal resolution of 2.5° × 1.9° with 26 vertical levels), and UCLA was run at the T62L28 resolution (close to 2.5° × 2° with 28 vertical levels).

The vegetation cover in the Control simulations for CAM5 and RegCM is specified according to the default CLM land cover for present-day conditions (Lawrence and Chase 2007) and in UCLA is based on Xue et al. (2004b). In the land cover change experiments, a degraded vegetation cover is specified. The type and magnitude of land cover changes applied to the RegCM are shown in Fig. 1. The land cover changes applied to CAM5 is the same as in Fig. 1 (but at the CAM5 resolution). The land cover changes in UCLA are similar but differ slightly due to differences in how vegetation is represented between the two models. The degraded areas cover the Sahel region north of 10°N and west of 35°E, and the Guinea Coast region between 0 and 10°W. In grid cells dominated by trees and shrubs in the Control, woody plants are replaced by grassland for up to 30 % of each grid cell (referred to as deforestation in this section) in LUC; in grid cells dominated by grassland in the Control, grass cover is replaced by bare soil for up to 30 % of each grid cell (referred to as desertification in this section) in LUC; over grid cells where woody plants and grass co-exist, desertification is applied only where deforestation is below 30 %, and the total area of deforestation and desertification combined do not exceed 30 % of each grid cell. The crop area fraction stays the same between Control and LUC. Therefore, land cover degradation influences no more than 30 % of each grid cell within the perturbation zone. This magnitude and spatial pattern of land cover changes follow the WAMME2 protocol, and are qualitatively consistent with the differences between the 1950s and 1990s based on the reconstructed historical land cover data from Hurtt et al. (2011). Therefore the land cover specified in Control and LUC are considered representative of the 1950s and 1980s, respectively. The 30 % upper limit of land cover change compares favorably with the estimated rate of deforestation (which was approximately 1–1.5 % per year as used in Paeth and Thamm 2007; Paeth et al. 2009).

The leaf area index (LAI) changes resulting from the prescribed land cover changes are shown in Fig. 2a, b. Over most of the perturbation zone, LAI decreases by no more than 1.0. In addition, soil color is modified slightly to represent the effect of soil erosion that often accompanies the degradation of vegetation cover. The changes of vegetation coverage, LAI and soil color together result in an increase of albedo that is in the range of 0.02–0.1 over most of the degraded areas (Fig. 2c, d), with a spatial average of approximately 0.06.

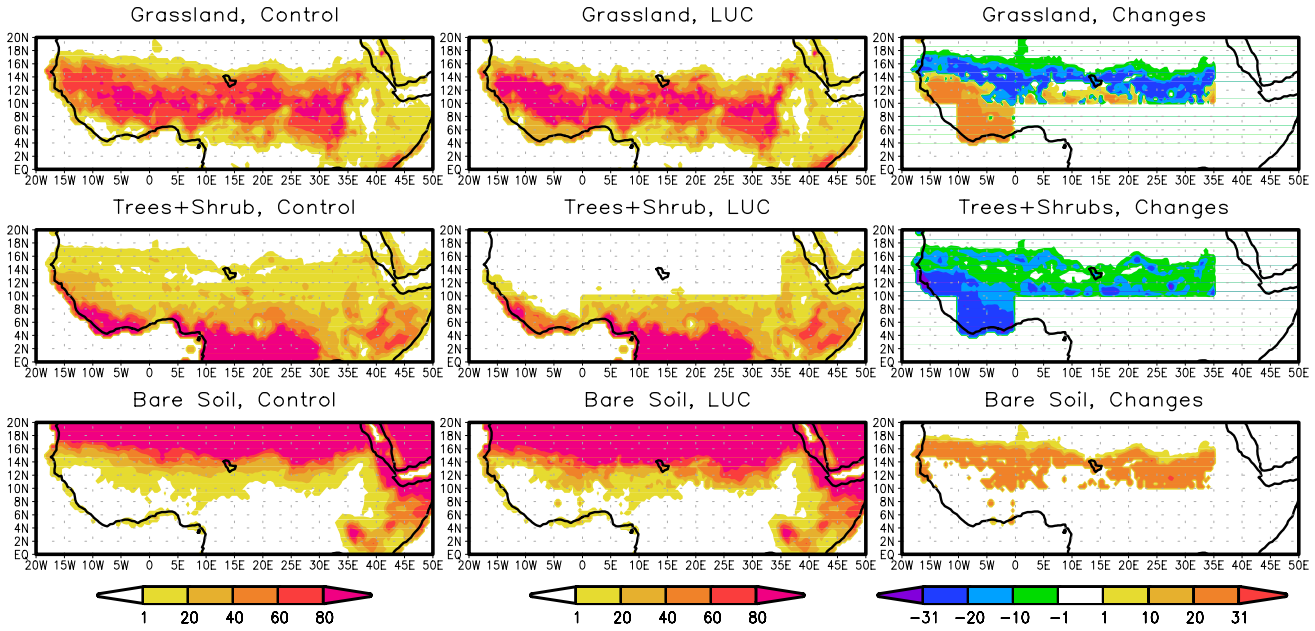

Fig. 1 Fractional coverage (in %) of different land covers prescribed in the Control simulation and LUC experiment, and the difference between the two (LUC–Control): grass (*top row*), trees and shrubs (*middle*), and bare soil (*bottom row*)

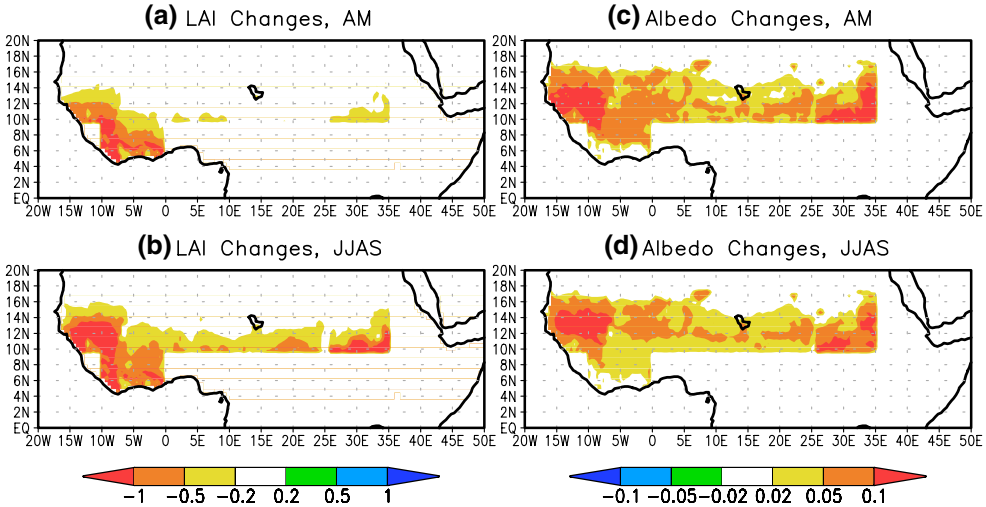

Fig. 2 LAI and albedo changes from Control to LUC, in the pre-monsoon season (April and May, *upper*) and during the monsoon (June–September, *lower*)

Three observational datasets are used in this study for comparison with model results, including: (1) the University of Delaware (UDel) monthly precipitation and temperature data (Legates and Willmott 1990; Willmott and Matsuura 1995), which is at a 0.5° spatial resolution and covers the period from 1901 on; (2) the NOAA Climate Prediction Center's global gauge-based analysis of monthly precipitation data (referred to as GTS in this study) (Chen et al. 2002), which dates back to 1948 with a spatial resolution of 1°; and (3) the monthly temperature data from the CPC Climate Anomalies Monitoring System (CAMS, Fan and van den Dool 2008), which dates back to 1948 with a 0.5° spatial resolution.

3 Model performance

To assess the performance of various models, precipitation in RegCM(R2) Control is compared against both the GTS data and the UDel data averaged over the 2002–2006

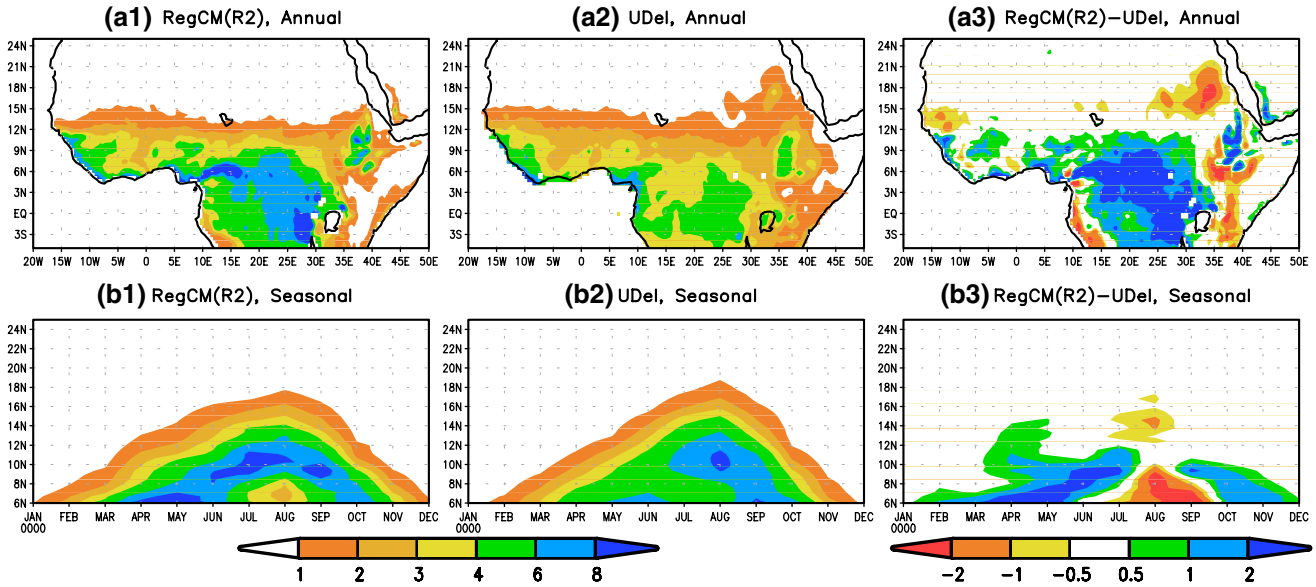

Fig. 3 Precipitation annual average (*upper*) and the seasonal cycle of zonally (10°W–10°E) averaged precipitation (*lower*), from RegCM(R2) (*left*), the UDel data (*middle*), and their differences (*right*)

period, and precipitation simulated by the GCMs in the last year of the Control simulations and the GCM-driven RegCM are compared against the long-term climatology of the GTS and UDel data. The model biases defined using these two different datasets are very similar. We therefore only present comparison with the UDel data. Figures 3 and 4 show these comparisons for both the annual average precipitation over Tropical Africa and the seasonal cycle of precipitation averaged over 10°W–10°E in West Africa.

Overall, RegCM(R2) captures the spatiotemporal variability of precipitation in West Africa quite well (Fig. 3), including the strong precipitation gradient in the latitudinal direction, location of precipitation maximum, and the abrupt northward shift of the rain belt center from the coast region to approximately 10°N at the monsoon onset in June. Over the West African sub-region (15W–10E, 6N–18N), the average root mean square error (RSME) of annual average precipitation is 0.63 mm/day, and the spatial correlation between model and observation is 0.94 (Table 2); however, the model overestimates precipitation during the pre-monsoon and post-monsoon seasons. In addition, during the peak monsoon season, the rain belt has a wet bias in southern Sahel and a dry bias in the coastal region. In August, the model rainfall does not extend sufficiently north. By and large, the spatial extent and seasonal evolution of precipitation in West Africa are properly simulated. Elsewhere in Tropical Africa, RegCM(R2) has a large wet bias over Central Africa and some dry bias in portions of East Africa.

Precipitation from both GCMs contains a well-defined spatial bias in West Africa (Fig. 4). CAM5 performs well in simulating annual precipitation in the southern part of West Africa and in Central Africa, but significantly overestimates annual precipitation in the north. The rain belt during the peak monsoon is located further north than observed; the resulting dry bias in the south balances the wet bias in the rest of the year, leading to a good agreement of annual precipitation with observations. The UCLA GCM has a strong wet bias in the southern part of West Africa, with an insufficient northward penetration of the monsoon during the peak monsoon, leading to a dry bias in the north.

Neither RegCM(CAM5) nor RegCM(UCLA) produces the same spatial biases of precipitation as their driving GCMs (Fig. 4). For CAM5, the dynamic downscaling significantly reduces the wet bias but enhances the dry bias along the coast; for UCLA, the dynamic downscaling reverses the north–south contrast of the model bias during the peak monsoon. The underestimation of precipitation over the coastal region during the peak monsoon seems to be a feature intrinsic to the RegCM that is independent of the driving GCM.

Based on the RMSE and the correlation coefficient (Table 2), the R2-driven RegCM outperforms both the GCMs and the GCMs-driven RegCM, which is not surprising as it has the most realistic LBCs. Overall, when measured by these commonly used performance metrics, the GCM-driven RegCM simulations do not seem to offer strong advantage over the driving GCMs in reproducing the present-day climate. This may be due to the lack of strong land surface heterogeneity and lack of complex topography in this region, and is therefore likely to be region-specific. The GCM-driven RegCM RMSEs are

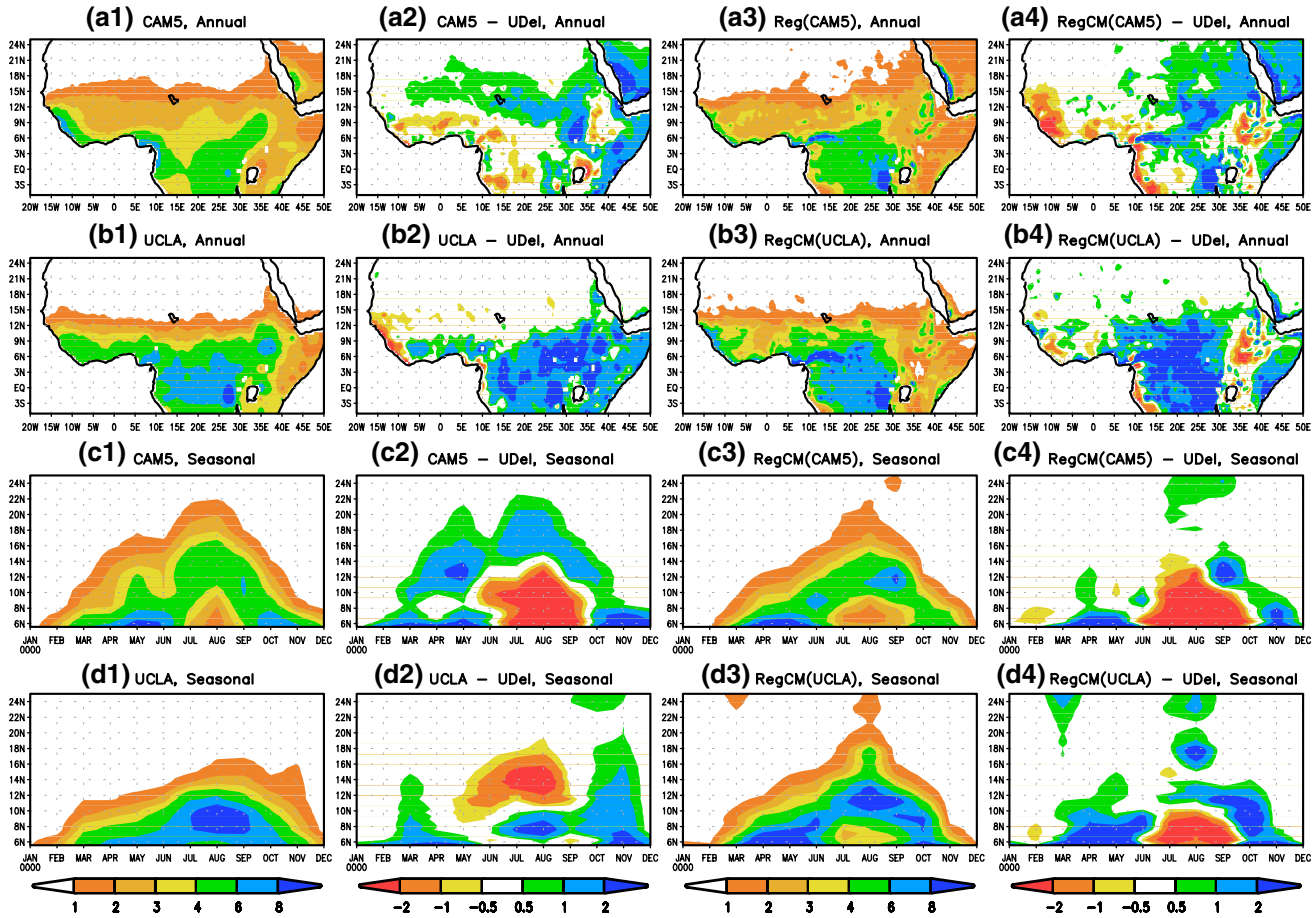

Fig. 4 The annual average precipitation and zonally averaged (10°W–10°E) seasonal cycle of precipitation (mm/day) simulated by CAM5, RegCM(CAM5), UCLA, and RegCM(UCLA) Control simulations and their difference from the UDel long-term climatology (which differs slightly from the UDel 6 year average shown in Fig. 3). Note that GCMs output from the last year of simulations are used here for consistency with the GCMs-driven RegCM results

Table 2 Performance matrix based on the comparison of annual precipitation between the Control simulation of each model and the UDel precipitation data over the West African sub-region (15W–10E, 6N–18N)

Models	RMSE (mm/day)	Corr. coeff.
RegCM(R2)	0.63	0.94
CAM5/RegCM(CAM5)	0.59/0.82	0.93/0.88
UCLA/RegCM(UCLA)	0.73/0.74	0.89/0.91

Note that results from the last year of the GCMs simulations are presented here for consistency with the GCMs-driven RegCM results; RegCM(R2) results are based on 5-year averages

either similar to or slightly larger than the corresponding GCM values; the spatial correlation with observation is lower in RegCM(CAM5) than in CAM5 but is higher in RegCM(UCLA) than in UCLA. Nevertheless, the regional model partially corrects a strong spatial bias found in the driving GCMs in West Africa.

4 Impact of land cover degradation on regional climate

This section focuses on documenting and understanding the response of model climate to land cover degradation. Differences among results from multiple models and from experiments using multiple approaches necessitate assessment of the model results against observational data. This is a challenging task due to the difficulty of separating the impact of land cover changes from other factors in observations. In the real world, actual precipitation and temperature changes result from a combination of large scale forcing (such as sea surface temperature and greenhouse gas concentration changes) and local surface condition changes. Nevertheless, comparison with observed precipitation changes may offer some suggestive evidence. The late twentieth century Sahel drought commenced in the 1960s and persisted for over three decades. We therefore use the observed difference between

the wet 1950s and the dry 1980s as the benchmark for models to compare against.

4.1 Model simulated precipitation changes

The impacts of land cover degradation on precipitation as simulated by CAM5 and UCLA are shown in Fig. 5 based on results from the last year of the model simulations. The 5-year averages of the model results follow a similar but smoothed spatial pattern with a smaller magnitude (results not shown). Here the last year is shown for comparison with the RegCM results driven by LBCs from the last year of the GCM runs. Both GCMs produce a predominantly dry signal in West Africa in response to the prescribed land cover degradation, with the signal fluctuating from month to month in CAM5 but showing a remarkable seasonal persistency in UCLA (Fig. 5a1, b1). Also, the two models produce very different spatial patterns of precipitation response. The reduction of precipitation occurs primarily in the Sahel region with the maximum reduction around 12°N in CAM5, but in UCLA it covers West Africa mostly south of 12°N and is also much larger in magnitude (Fig. 5a1, b1). This statement holds for both the pre-monsoon season (April and May, "AM" hereafter) (Fig. 5a2, b2) and the monsoon season (June, July, August, and September, "JJAS" hereafter) (Fig. 5a3, b3). In addition, during both seasons in CAM5, the precipitation response to land cover degradation shows a clear dipole pattern in West Africa, with a dry signal over the Sahel and wet signal over the Guinea Coast; UCLA does not produce a clear dipole pattern over land. In Central Africa over the Congo forest region, both models produce a wet signal in JJAS, but the two models contradict each other in the pre-monsoon season, with a strong wet signal in CAM5 and a strong dry signal in UCLA.

The response of precipitation to land cover changes as simulated by RegCM driven with different LBCs is shown in Fig. 6. Note that the results shown in the top three rows are from simulations based on the LUC approach in which the land cover degradation experiment uses the same set of LBCs as the corresponding control (derived from

Fig. 6 Precipitation changes (in mm/day) induced by land cover changes as simulated by RegCM(R2) (*1st row*), RegCM(CAM5) LUC approach (*2nd row*), RegCM(UCLA) LUC approach (*3rd row*), RegCM(CAM5) LUC2 approach (*4th row*), and RegCM(UCLA) LUC2 approach (*5th row*): seasonal cycle of precipitation changes averaged over 10W–10E north of 5N (*left*); spatial distribution of precipitation changes averaged during the pre-monsoon season (*middle*) and monsoon season (*right*)

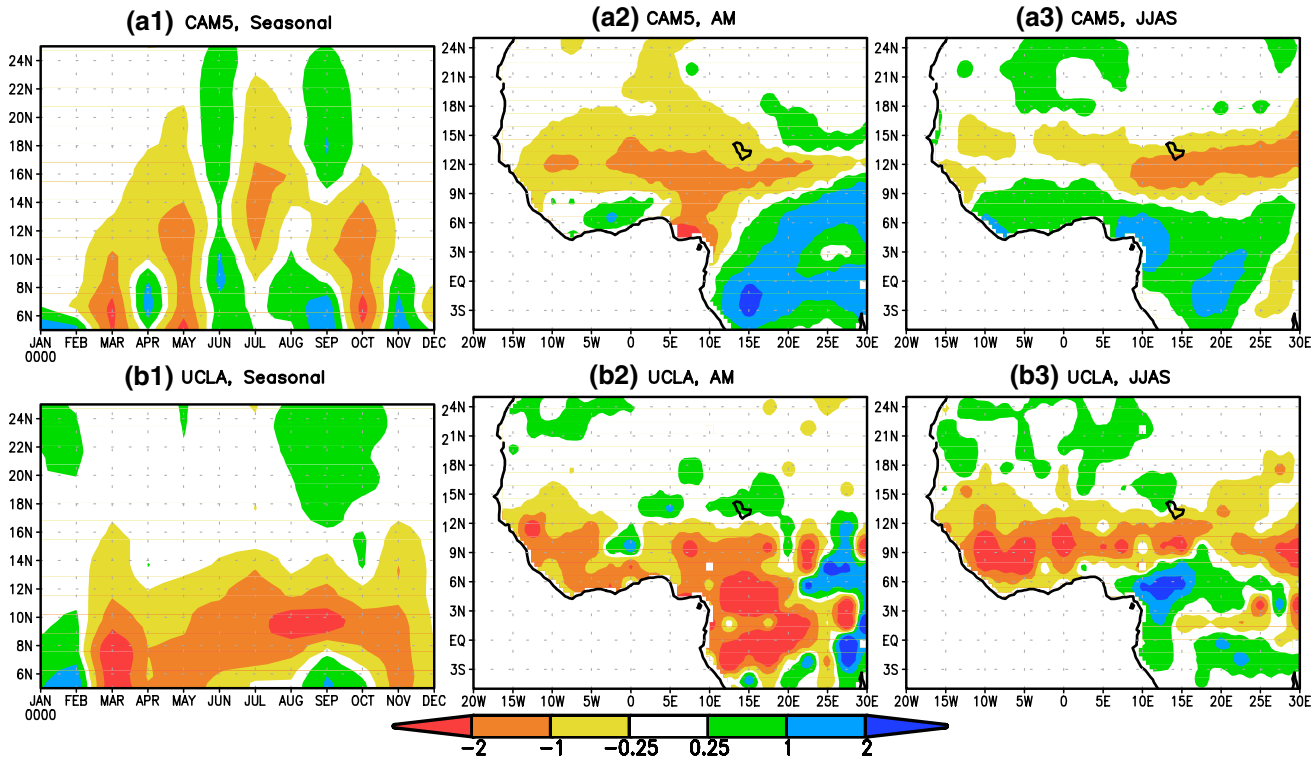

Fig. 5 LUC-induced precipitation changes (mm/day) simulated by CAM5 (*upper*) and UCLA GCM (*lower*) based on model output from the last year of simulations: Seasonal cycle of zonal average over 10°W–10°E (**a1**, **b1**), average during the pre-monsoon season (**a2**, **b2**) and average during the monsoon season (**a3**, **b3**)

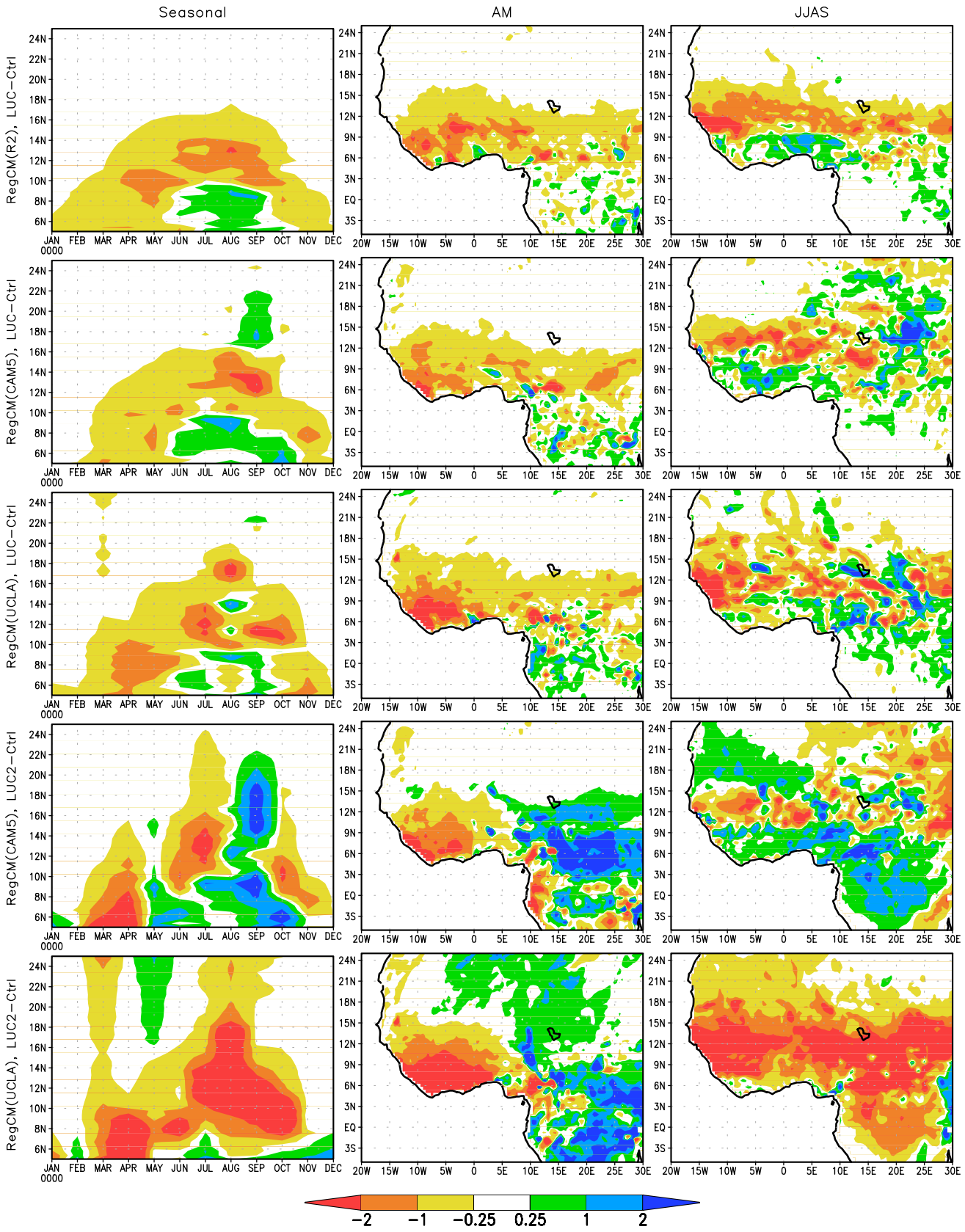
Seasonal
AM
JJAS
RegCM(R2), LUC−Ctrl
RegCM(CAM5), LUC−Ctrl
RegCM(UCLA), LUC−Ctrl
RegCM(CAM5), LUC2−Ctrl
RegCM(UCLA), LUC2−Ctrl
JAN FEB MAR APR MAY JUN JUL AUG SEP OCT NOV DEC
0000
−2 −1 −0.25 0.25 1 2

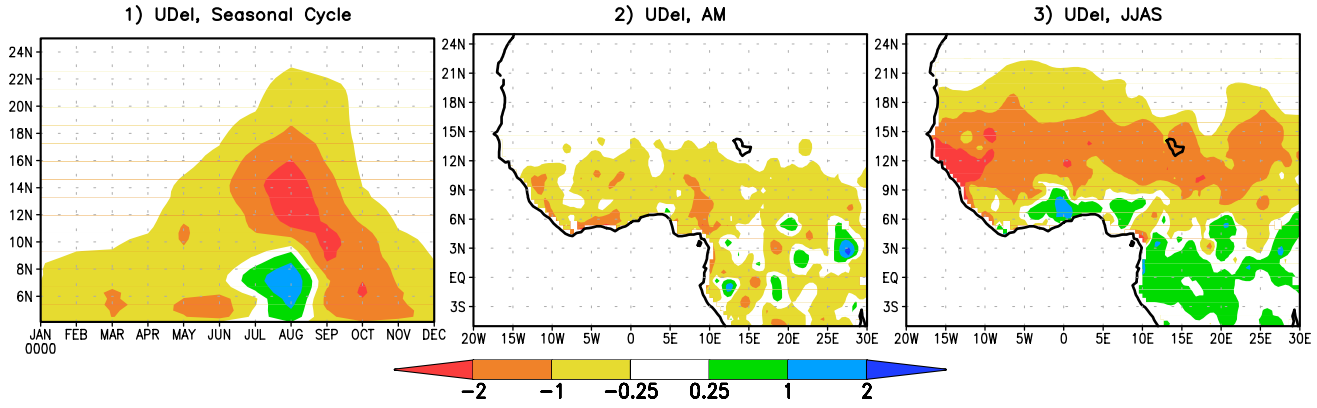

Fig. 7 Precipitation difference between 1950s and 1980s based on the UDel data: **1** Seasonal cycle of zonal average over 10°W–10°E, north of 5N; **2** Spatial distribution averaged during the pre-monsoon season (April and May) and **3** during the monsoon season (June–September)

reanalysis data or a GCM Control simulation). With this approach, results from all three models [i.e., RegCM(R2), RegCM(CAM5), and RegCM(UCLA)] are remarkably similar, including a clear decrease over most of West Africa, a slight increase over Guinea Coast during the peak monsoon, and a mixed signal or slight increase in Central Africa. Throughout the year, a general decrease of precipitation is found in West Africa. During AM, the decrease of precipitation is spatially coherent in West Africa in all three models, with stronger decrease close to the coast, and the magnitude of the decrease exceeds 2 mm/day in some areas. During JJAS, the strongest decrease of precipitation is centered along 12°N. Land cover degradation is found to cause a weakening of the monsoon circulation in the models, leading to a southward shift of the rain belt and therefore a dipole pattern of precipitation response during JJAS, with a decrease over the Sahel and an increase over the Guinea Coast region and Central Africa. In addition to the dipole pattern, the precipitation response shows a higher degree of spatial heterogeneity during JJAS than during AM, especially from the GCMs-driven simulations. The stronger heterogeneity in the GCMs-driven RegCM may be partly due to the use of only 1 year of data while results from RegCM(R2) is the average of 5 years. Overall, there is no qualitative difference in the spatial and seasonal patterns of precipitation response to land cover degradation between RegCM driven with different GCMs and RegCM driven with reanalysis data. It seems that when the LUC approach is used, different LBCs of the regional climate model do not have any substantial impact on the simulated effect of land cover change.

Results shown in the lower two rows of Fig. 6 are based on the LUC2 approach in which the RegCM LBCs for the land cover degradation experiment (LUC2 in Table 1) are derived from the corresponding LUC experiment of CAM5 or UCLA and therefore differ from the LBCs of the corresponding Control simulation. With this methodology, the spatial and seasonal patterns of the precipitation response differ substantially between the two models, and differ substantially from those based on the LUC approach as well. With the LUC2 approach and during the JJAS season, RegCM(UCLA) produces an extremely strong and spatially coherent dry signal, while a strong wet signal is found over most of West and Central Africa in RegCM(CAM5). The only dry signal in RegCM(CAM5) during JJAS over West Africa is found over a band along 12°N. During the AM season, the two models agree well, with a strong dry signal in West Africa and a strong wet signal east of 10°E.

Comparison between Fig. 5 and the lower two rows in Fig. 6 reveals several interesting points. First, for the seasonal and spatial patterns, the land cover change impact simulated by the regional climate model using the LUC2 approach are dominated by signals from the driving GCMs. In the annual cycle, the seasonal oscillations in RegCM(CAM5) and the seasonal persistence in RegCM (UCLA) reflect the RCM's downscaling nature, but the magnitude of the response and detailed spatial characteristics tend to be modified by the regional model. Meanwhile, over Central Africa in both seasons, the RegCM(UCLA) and UCLA produce precipitation responses of opposite directions. Second, during the JJAS season, the strongest decrease of precipitation in West Africa is located along 12°N in all RegCM simulations, regardless of the LBCs and approaches used. This is especially conspicuous in the contrast between UCLA (for which the maximum signal is along 8°N) and RegCM(UCLA).

4.2 Comparison with observed precipitation differences

Precipitation anomalies associated with the late twentieth century Sahel drought, defined as the precipitation

difference between the dry 1980s and the wet 1950s based on the UDel data, are shown in Fig. 7. Results from the GTS data (not shown) are similar. In the peak monsoon season JJAS, the observed drought featured a strong dry signal in the Sahel paired with a wet signal along the Guinea Coast and in Central Africa; in other seasons a dry signal is dominant across West Africa.

Compared with the land-induced precipitation changes in global and regional models shown in Figs. 5 and 6, both the magnitude and the overall spatiotemporal distribution of observed precipitation difference between 1950s and 1980s (Fig. 7) more closely resemble those from the RegCM LUC experiments than those from the GCMs experiments and the RegCM LUC2 experiments, although they all produce drought signals in the Sahel. These results suggest that, with the experimental design used in this study, the regional climate model with the LUC approach performs better than the same model with the LUC2 approach and better than the GCMs in capturing the precipitation response.

The comparison of precipitation response to land cover changes between RegCM LUC and GCMs is especially interesting, since the regional model (with results from just 1 year) does not seem to outperform the driving GCMs in capturing the precipitation climatology in the Control simulations (Table 2). During the AM season, CAM5 simulates a dipole pattern of precipitation response that is not in the observed changes, but RegCM(CAM5) does not have this problem; UCLA simulates too strong a drought that extends to Central Africa, but RegCM(UCLA) seems to correct this extreme strong signal. During the JJAS season, CAM5 places the strongest drought signal in eastern Sahel, while RegCM(CAM5) places the strongest drought signal in western Sahel consistent with observed changes; UCLA produces some increase of precipitation over the ocean with no clear dipole pattern of precipitation response over land in West Africa, while RegCM(UCLA) places the dipole pattern over land consistent with observed changes. Table 3 shows that using the observational difference between the 1980s and the 1950s as benchmark, the RegCM LUC approach in general performs better than the GCMs and better than the RegCM LUC2 approach. Possible reasons for this performance difference will be discussed in Sect. 5.

4.3 Model-simulated temperature changes

Similar to the impact on precipitation, the impacts of land cover degradation on surface air temperature in West Africa simulated by RegCM(R2), RegCM(CAM5), and RegCM(UCLA) using the LUC approach agrees with each other fairly well (top three rows in Fig. 8). The land-induced changes in temperature are small, and the signal shows a south–north dipole pattern that reverses between wet and dry seasons. In general, the RegCM LUC approach produces a warming signal in wet seasons/regions and a cooling signal in dry seasons/regions, and the strongest warming coincides with the strong decrease of precipitation. Over most areas of land cover degradation during the AM season, a warming is simulated by all three models; during the JJAS season, all three models produce a warming signal over the Sahel and a cooling signal to the south, forming a dipole pattern that resembles that of the precipitation response (Fig. 6).

Surface temperature response to the same amount of land cover changes simulated using the LUC2 approach (bottom two rows in Fig. 8) is drastically different from that based on

Table 3 The land-induced precipitation changes (in mm/day) simulated by each model averaged in specific seasons and sub-regions, and the corresponding 1980s minus 1950s precipitation differences (in mm/day) based on the UDel data

Methodology/models and data	Sahel-west (9–17N, 15W–15E)		Sahel-east (9–17N, 15E–30E)		Guinea coast (5–9N, 5W–10E)		Central Africa (5S–5N, 10E–30E)		RMSD
	AM	JJAS	AM	JJAS	AM	JJAS	AM	JJAS	
UDel data	−0.31	−1.39	−0.17	−1.02	−0.69	0.15	−0.29	0.26	–
GCMs									
CAM5	−0.81	−0.32	−0.15	−0.80	−0.46	0.60	0.97	0.50	0.65
UCLA	−0.36	−0.77	−0.08	−0.66	−1.15	−0.54	−1.05	0.22	0.47
RCM LUC approach									
RegCM(R2)	−0.57	−0.90	−0.28	−0.53	−0.72	0.53	0.03	0.10	0.32
RegCM(CAM5)	−0.44	−0.68	−0.22	0.36	−0.56	0.43	0.05	0.02	0.58
RegCM(UCLA)	−0.53	−0.84	−0.32	−0.29	−0.85	0.17	0.10	0.17	0.37
RCM LUC2 approach									
RegCM(CAM5)	−0.12	−0.12	0.55	−0.33	−0.42	0.81	0.39	0.54	0.68
RegCM(UCLA)	−0.34	−2.58	0.22	−2.51	−2.03	−0.83	1.10	−0.73	1.09

The RMSD (mm/day) for each model is calculated based on the difference between precipitation changes from each model and from UDel data in the seasonal and regional averages listed in this table

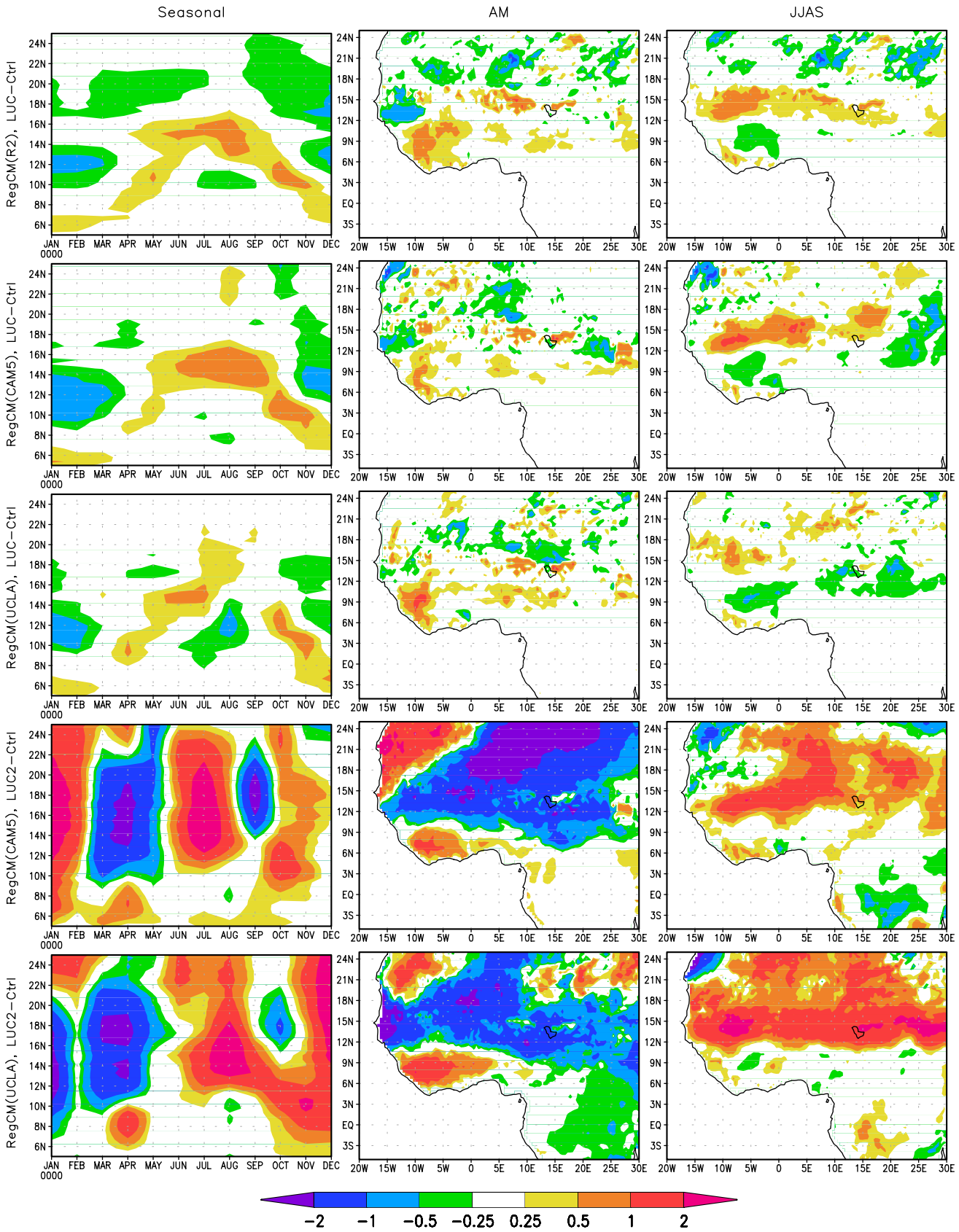

Fig. 8 Similar to Fig. 6, but for 2-m air temperature changes

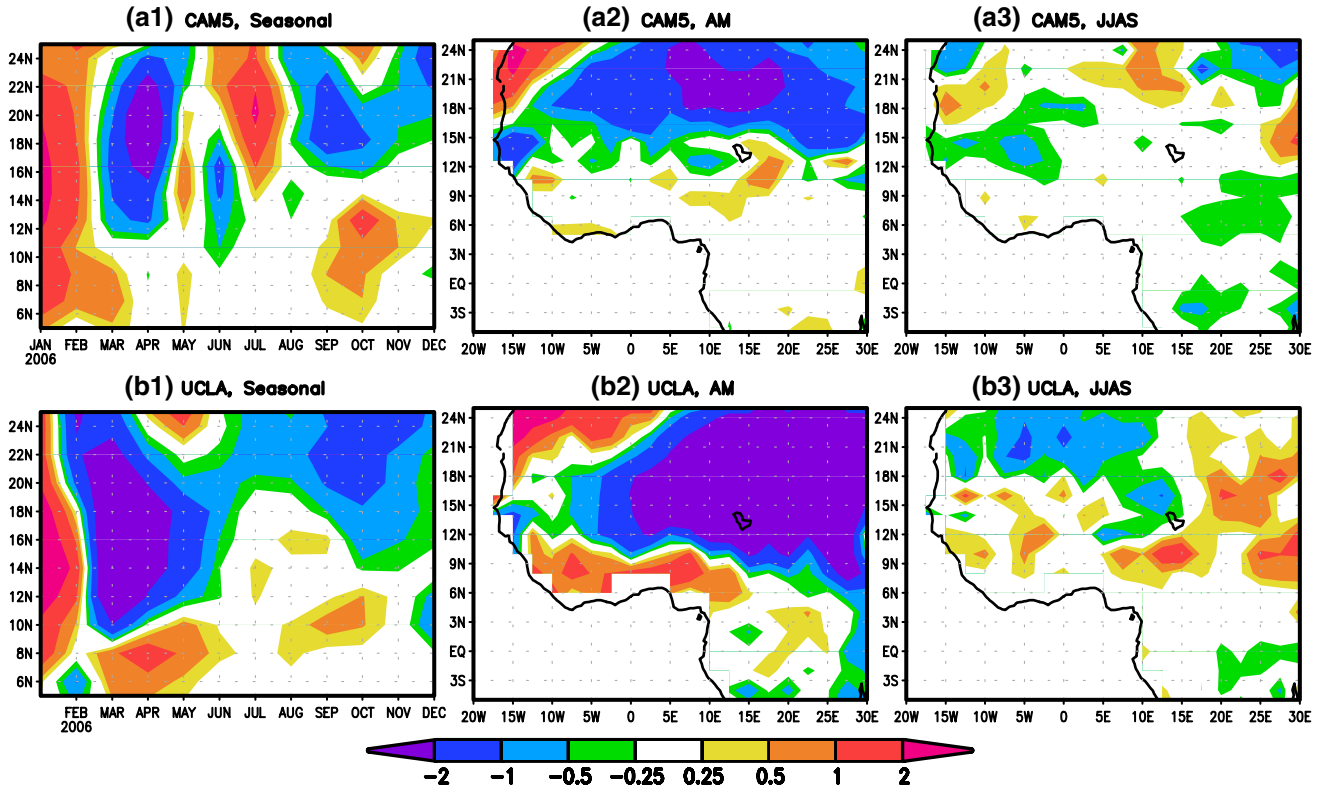

Fig. 9 Similar to Fig. 5, but for 2-m air temperature changes

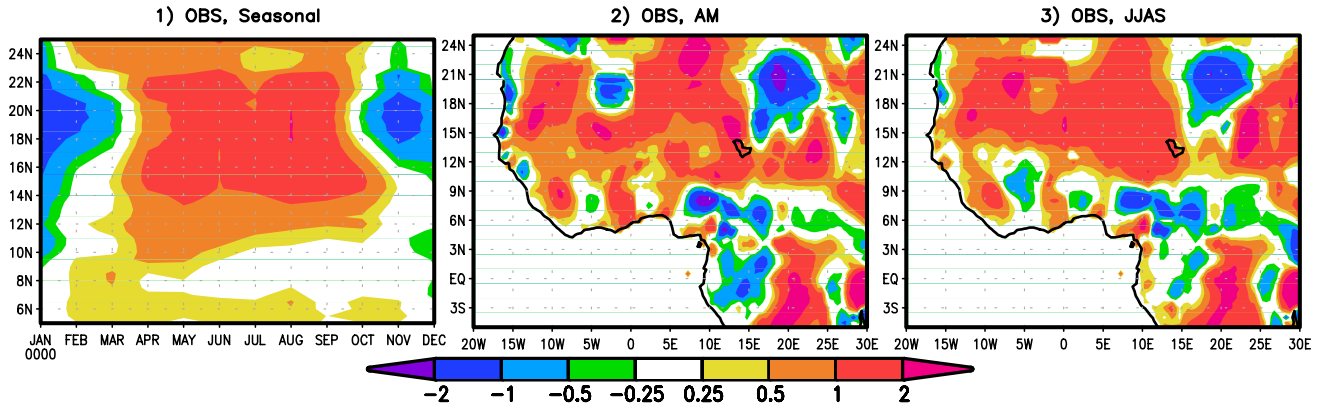

Fig. 10 Observed temperature differences between 1980s and 1950s, based on the CAMS data

the LUC approach. The magnitude of temperature changes is much larger, and the direction of temperature changes shows oscillations with no well-defined seasonal pattern. In the pre-monsoon season, both RegCM(CAM5) LUC2 and RegCM(UCLA) LUC2 experiments produce a warming signal limited to the Guinea Coast region, with strong and spatially extensive cooling over the Sahel and to the north; in the JJAS season, a strong and spatially extensive warming signal is simulated over the Sahel and to the north. The generally large magnitude of temperature response and the strong pre-monsoon cooling in the LUC2 experiments during AM seem to have originated from the response in the GCMs (Fig. 9). During the JJAS season however, a modest warming signal in the GCMs is vastly amplified in the RegCM LUC2 experiments (Fig. 8). Qualitatively, neither of the GCMs can produce the dipole pattern of Sahelian warming and Guinea Coast cooling, a characteristic response of RegCM especially when based on the LUC approach.

4.4 Comparison with observed temperature differences

Figure 10 shows the observed temperature differences between 1980s and 1950s based on the CAMS data. The temperature differences based on the UDel data are almost identical (results not shown). Due to the existence of greenhouse gas warming that dominates the past temperature trend across the globe, comparison of the model-produced temperature response to LUC with observed temperature changes is more complicated than a similar comparison for precipitation. Nevertheless, several findings are worth mentioning. First, the observed data shows a distinct seasonality of temperature changes in West Africa, with warming over most part of the year and cooling during the winter season; second, the observed temperature changes during JJAS feature a dipole pattern over West Africa, with strong warming in the north and weak cooling in the south. Both features are consistent with results from RegCM based on the LUC approach. This agreement would not be jeopardized (and instead would be enhanced) if a uniform warming (representing the impact of greenhouse gas impact) were to be deducted from the observed temperature differences. Nevertheless, all the experiment results here suggest that land cover change might have contributed to the observed warming during the summer monsoon season.

4.5 Mechanisms underlying the impact of land degradation

To help understand the RegCM-simulated climate response to land cover changes, the surface energy and water budgets are analyzed here focusing on the AM and JJAS seasons.

Figures 11 and 12 compare precipitation changes with changes in local and non-local moisture supplies, i.e., evapotranspiration (ET) and atmospheric moisture convergence, in the two seasons respectively. During the pre-monsoon season, the simulated precipitation decrease is dominated by a decrease of ET in the north and a decrease of atmospheric moisture convergence in the south when the LUC approach is used (the top three rows of Fig. 11). The ET decrease is limited to a small portion of the areas of land cover changes, and the spatial patterns of ET response and moisture convergence response are very similar across the three models [i.e., RegCM(R2), RegCM(CAM5), and RegCM(UCLA)]. When the LUC2 approach is used, the precipitation response is dominated by an ET decrease in the west and a moisture convergence increase in the east in both RegCM(CAM5) and RegCM(UCLA). During the monsoon season, the spatial distribution of precipitation changes is overwhelmingly dominated by changes in the atmospheric moisture convergence, regardless of which model and approach are used (Fig. 12).

The changes in atmospheric moisture convergence reflect changes in regional circulation, which results from changes in temperature gradient; and the latter is strongly influence by ET. As shown in Figs. 11 and 12, across all RegCM simulations and in both seasons, the primary signal of local ET response is a decrease. Two factors contribute to this response to vegetation degradation: the decrease of evaporating and transpiring leaf areas (which leads to a higher Bowen ratio with a partition of net radiation towards more sensible heat flux) and the decrease of surface roughness therefore drag coefficient (which tends to reduce both sensible and latent heat fluxes). The changes of surface net radiation (Fig. 13) share a similar spatial pattern with the ET changes in both seasons, with a strong decrease across the region of land degradation in the pre-monsoon season, and a decrease over a band north of 12N in the Sahel and a slight increase in the south during the monsoon. The decrease of net radiation results primarily from the increase of surface albedo shown in Fig. 2. Over most areas of surface net radiation decrease in the LUC apporach, surface air temperature is found to increase (Fig. 8 vs. Fig. 13), due primarily to the decrease of evaporative cooling that dominates over the decrease of net radiation. However, over the Sahel region during the pre-monsoon season when the LUC2 approach is used, a strong cooling covers a major portion of the areas of surface net radiation decrease. This is primarily a result of advection of cool air from the north and northeast related to large scale circulation changes.

The LUC-induced temperature changes may play an important role in the model precipitation response through its impact on regional circulation, the African easterly jet (AEJ) in particular. AEJ, located around 600mb north of the monsoon trough, results from the positive meridional temperature gradient from the Guinea Coast to the Sahara desert. The RegCM driven by R2 LBCs captures the location of the AEJ based on comparison with the long-term climatology of the NCEP re-analysis data (Fig. 14), but underestimates the strength of AEJ. In fact, RegCM driven with all three different LBCs produces a very weak AEJ. Both the strength and location of AEJ can influence the atmospheric moisture convergence, therefore precipitation. A stronger AEJ or a southward shift of its location favors more precipitation over the Guinea Coast region and less precipitation over the Sahel (Cook 1999). During the monsoon season, the warming induced by land cover degradation over the Sahel region can enhance the positive meridional temperature gradient, leading to a stronger AEJ and potentially a southward displacement of AEJ. As shown in Fig. 14, with the LUC approach, RegCM driven with all three different LBCs produces a slightly stronger AEJ but no obvious southward shift of its location compared with the control; with the LUC2 approach however, the AEJ is much stronger and its location shows a southward

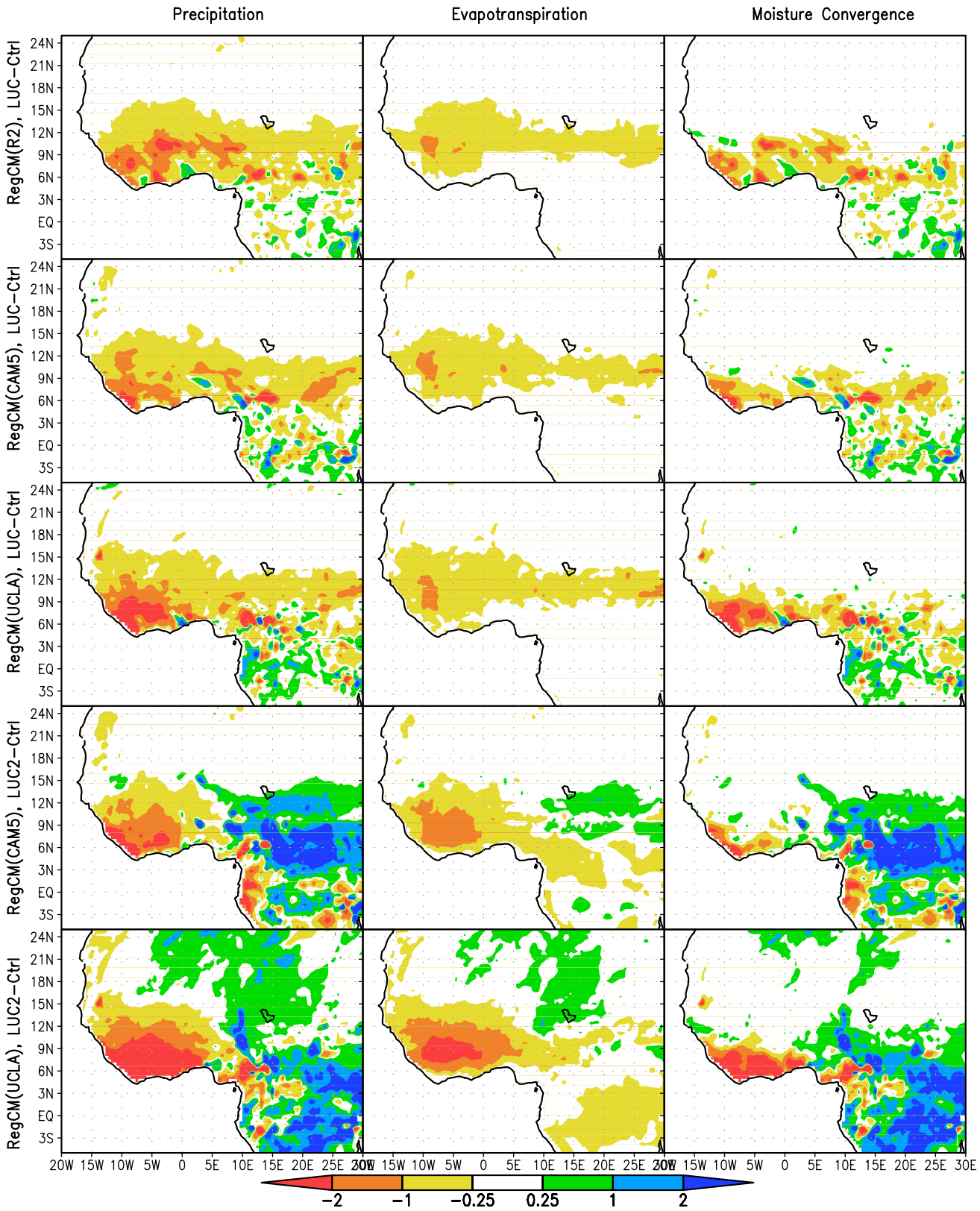

Fig. 11 Changes of pre-monsoon season (April and May) precipitation (*left*, in mm/day), evapotranspiration (*middle*, in mm/day), and moisture convergence (*right*, in mm/day) caused by land use land cover changes simulated by RegCM(R2) (*1st row*), RegCM(CAM5) LUC approach (*2nd row*), RegCM(UCLA) LUC approach (*3rd row*), RegCM(CAM5) LUC2 (*4th row*), and RegCM(UCLA) LUC2 approach (*5th row*). Note that the precipitation difference is the same as that shown in Fig. 6, repeated here to facilitate comparison

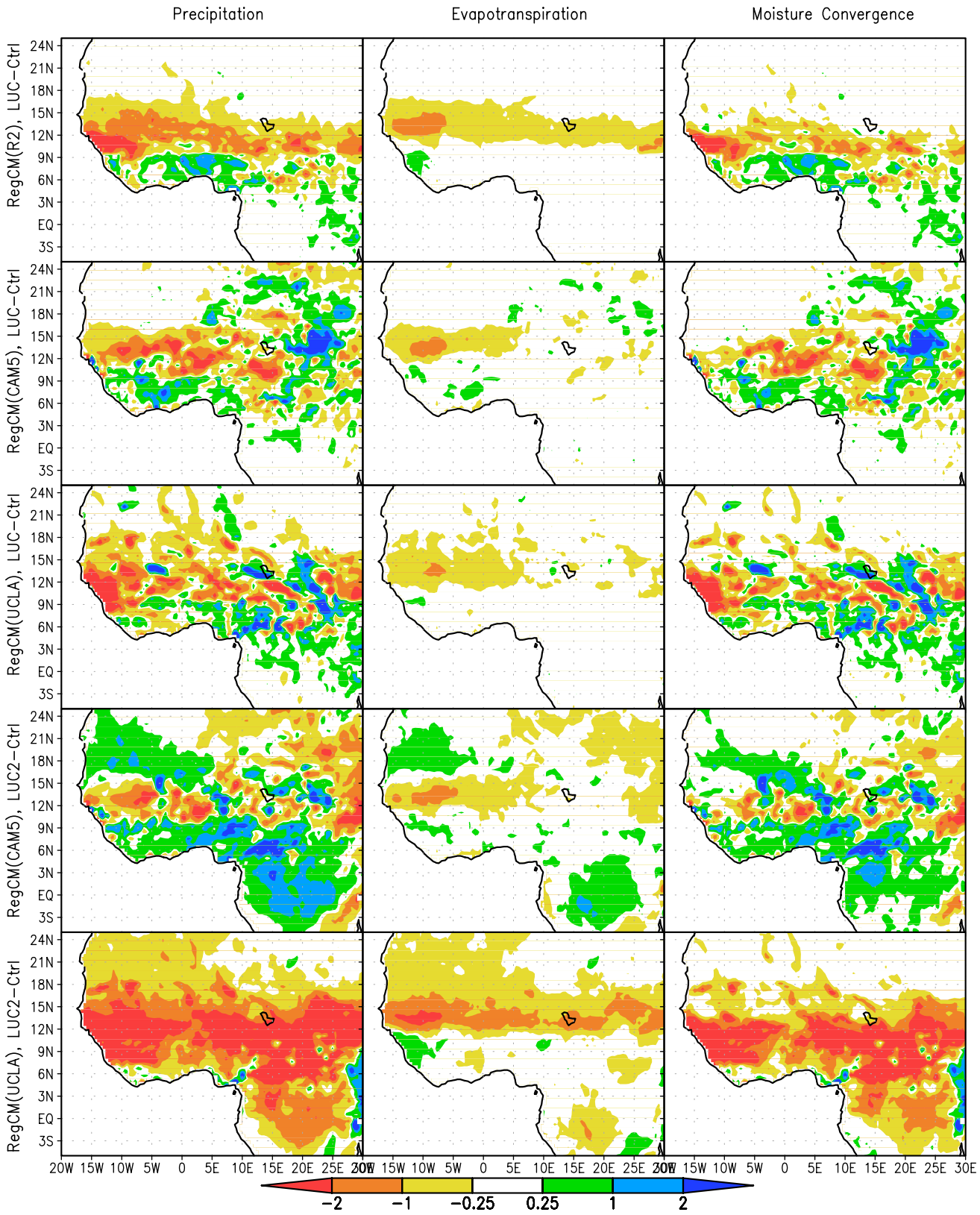

Fig. 12 Similar to Fig. 11, but for the JJAS season

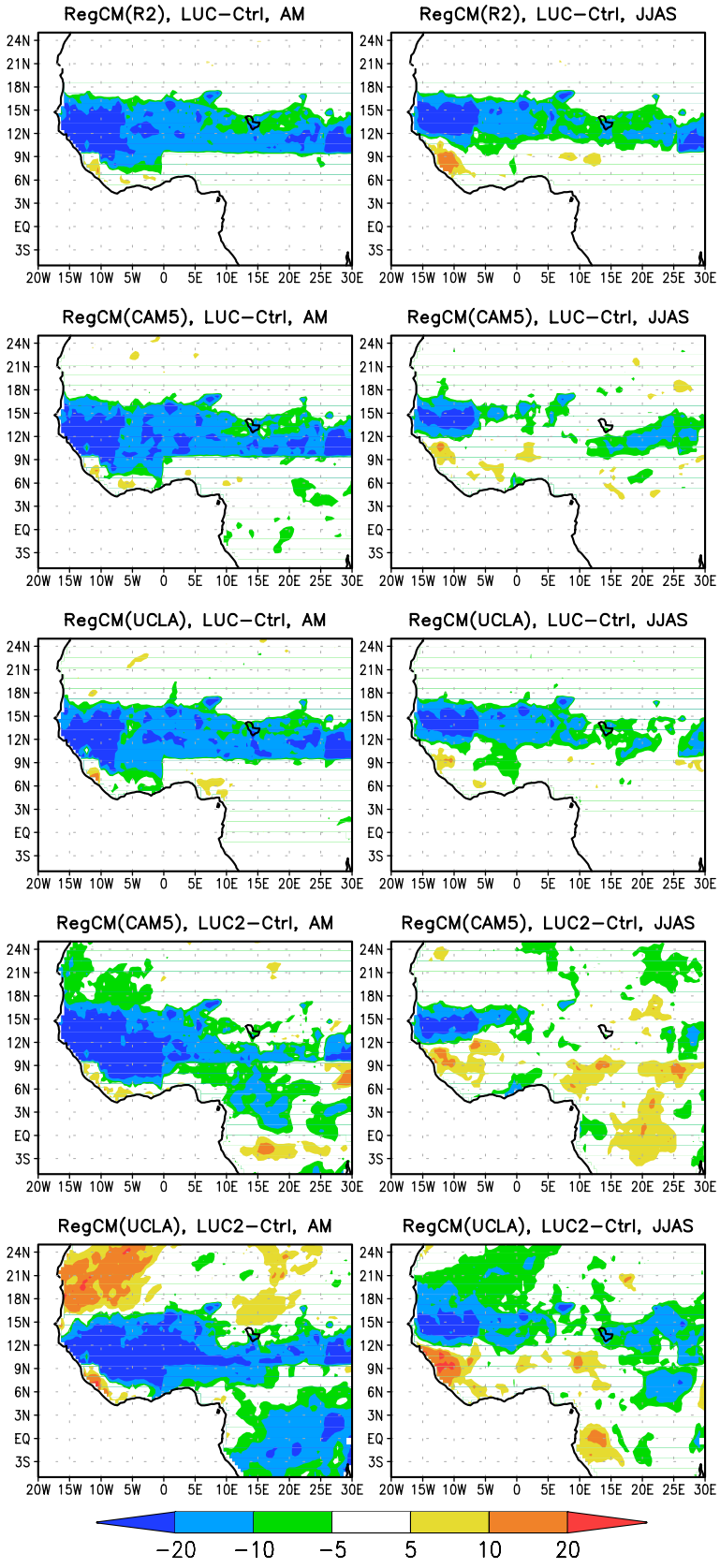

Fig. 13 LUC-induced surface net radiation changes (in W/m^2) during pre-monsoon (*left*) and monsoon (*right*) seasons, simulated using RegCM(R2), RegCM(CAM5) LUC approach, RegCM(UCLA) LUC approach, RegCM(CAM5) LUC2 approach, and RegCM(UCLA) LUC2 approach. Surface net radiation is defined positive downward

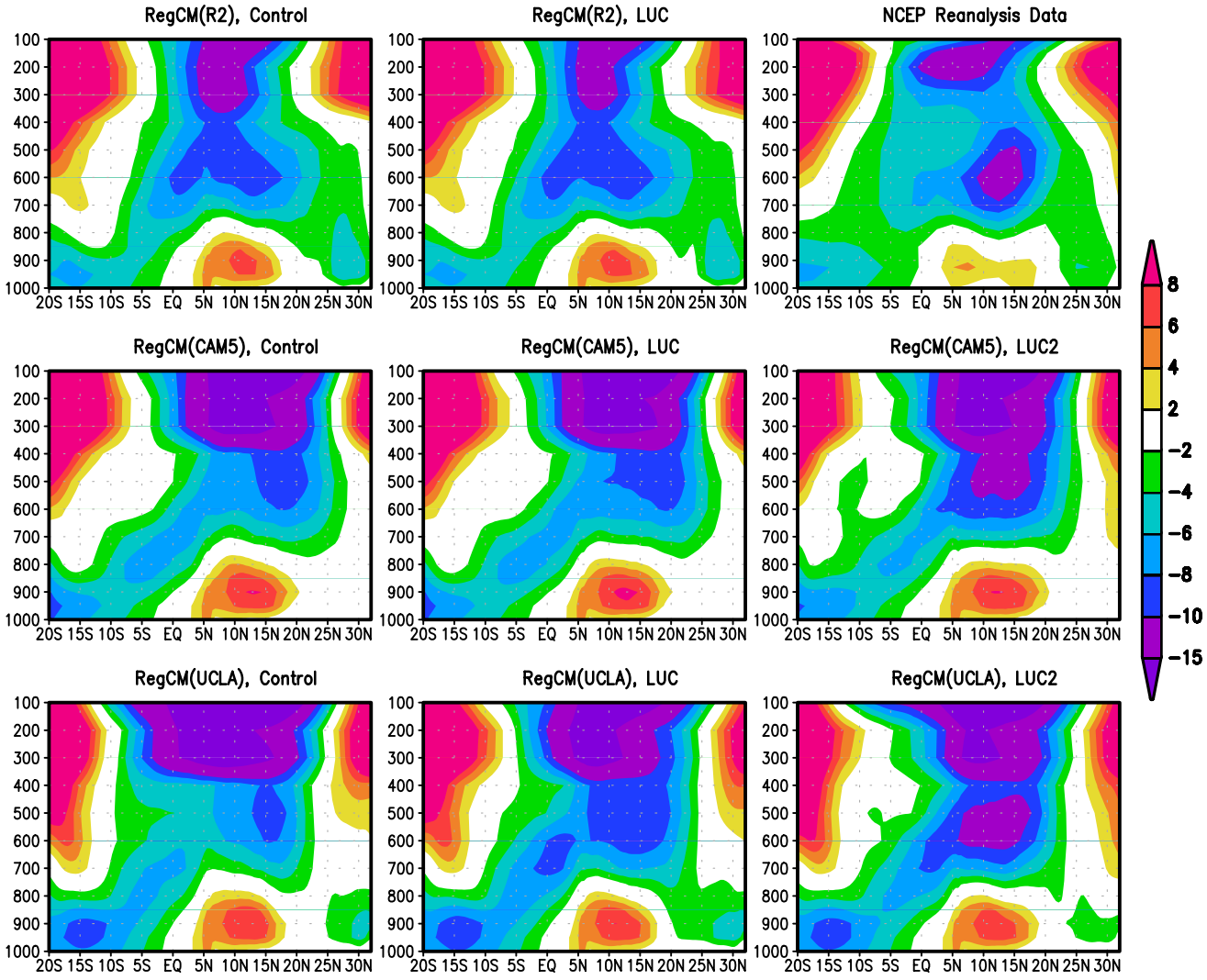

Fig. 14 Zonal wind at 0° longitude, averaged during JJA season for different simulations by the regional climate model

shift. This circulation response to land cover degradation in LUC2 is therefore consistent with an overall decrease of precipitation over the Sahel region and an increase over the Guinea Coast. With the LUC approach, the circulation changes in the land cover degradation experiments are largely constrained and weaker than the changes in the LUC2 experiment.

Overall, in the response of regional climate to changes in land cover, ET changes seem to play a more important role than albedo changes during the monsoon season. For temperature, the decrease of ET dominates over the albedo increase, leading to warming in the Sahel region. For precipitation, on one hand, the decrease of ET reduces local moisture supply to the monsoon system; on the other hand, it influences atmospheric moisture convergence through its impact on meridional temperature gradient therefore the strength and location of AEJ.

5 Summary and discussion

In an effort to understand the potential role of LUC in the late twentieth century Sahel drought, two GCMs (CAM5 and UCLA) and an RCM (RegCM) are used here to study the impact of "idealized-but-realistic" land cover changes on the regional climate in West Africa. The changes imposed on the model land cover roughly correspond to the land cover degradation from 1950s to 1980s in West Africa. Three different sources of LBCs are used to drive the RegCM, including the R2 reanalysis data and output from the two GCMs. Based on precipitation comparison between model control runs and the UDel data, RegCM driven by re-analysis data performs better than the GCMs-driven RegCM and better than both GCMs, and the GCMs-driven RegCM corrects or alleviates some spatial bias of precipitation in the driving GCMs.

Using the two GCMs, the GCMs-driven RegCM, and the R2-driven RegCM, the impact of land cover degradation was quantified based on paired control-and-experiment simulations that differ in land cover. For the RegCM experiments, two different approaches are tested: the LUC experiment is driven by the same LBCs as the corresponding Control simulation, which are from the R2 reanalysis or from the GCM Control simulation; the LUC2 experiment is driven by LBCs from the GCM land use change experiment. When the LUC approach is used, the RegCM-simulated impacts of land cover degradation on regional precipitation and surface temperature are robust across different sources of LBCs. The resulting changes include a precipitation decrease in most of West Africa throughout the year, and a general warming in the rainy season and cooling in the dry season. Over the Guinea Coast during the peak monsoon, a slight increase of precipitation and a general cooling are simulated, leading to a Sahel–Guinea dipole pattern for both precipitation and temperature changes. A slight increase of precipitation or mixed signal is simulated over Central Africa. The spatiotemporal distribution of changes in precipitation and temperature based on the RegCM LUC experiments are consistent with the observed changes associated with the late twentieth century Sahel drought. The LUC-induced precipitation changes in West Africa are dominated by changes in ET in the north and by changes in atmospheric moisture convergence in the south, and the latter is likely to have resulted from the ET impact on temperature gradient (therefore on the AEJ). For the LUC-induced temperature changes, warming caused by the decrease of evaporative cooling dominates over cooling caused by the radiative effect of surface albedo increase.

When the LUC2 approach is used, the response of precipitation and temperature in RegCM is dominated by the response in the driving GCMs, including an oscillation between dry and wet signals in the seasonal cycle and the pre-monsoon warming over the Guinea Coast and strong cooling in the north that was not observed. Some signals from the GCMs are drastically amplified in the regional model. Overall, relative to results from the RegCM experiment using the LUC approach, the precipitation response to land cover degradation simulated by the two GCMs and by the RegCM LUC2 approach are less consistent with the observed changes associated with the late twentieth century drought. However, the simulated AEJ changes in GCMs and in the GCMs-driven RegCM LUC2 experiments are more consistent with the observed pattern of precipitation changes, suggesting that the use of the same LBC in RegCM LUC may suppress the land cover change impact on regional circulation.

Theoretically, the RCM LUC2 approach has the advantage of capturing the effects of land cover changes on large-scale circulation. In a previous study over the U.S. region (Xue et al. 2012), with relative weak surface disturbance and land/atmosphere interaction taking place mostly through wave propagation, it was found that it was crucial to incorporate LBC changes as was done in LUC2 in this study. However, the LUC2 approach also suffers from disadvantages. As the performance of GCMs are generally not optimized for any specific region, its response to land cover changes in the specific region of interest may not be as accurate as that in an RCM. Through the LBCs, LUC2 inherits the impacts of any potential erroneous response of the driving GCM to land cover changes, and such effects from the GCM may get amplified in the RCM LUC2 experiment due to the frequent inconsistency between RCM and the driving GCM in physical parameterizations that influence the climate response to land cover changes. In addition, the LUC2 approach is also subject to the effects of GCMs' internal variability. Therefore, to derive the signal for land cover change impact using LUC2 approach, a large ensemble will be needed to reduce the uncertainties inherited from the driving GCMs. On the other hand, the disadvantage of the RCM LUC approach in not fully capturing the impact on large scale circulation will be less of a concern where the non-local impact of land cover changes is small or when the RCM domain is sufficiently large to capture the non-local impact. These are the possible reasons why the LUC approach performs better than the LUC2 approach based on the metrics used in this study. For general application, which approach is more appropriate will depend on the question to be addressed. The LUC approach may be preferred when the impact on the mean climate is concerned; the LUC2 approach will be necessary when it is important to capture the temporal variability.

Although our results suggest that land cover degradation of reasonable magnitude and spatial extent in the models are capable of triggering a drought comparable to the observed drought, it is likely that both large scale oceanic forcing and regional land cover changes are important contributing factors for the observed drought. The effects of oceanic forcing on the Sahelian drought were demonstrated in several studies based on results from individual GCMs (e.g., Giannini et al. 2003; Lu and Delworth 2005). However, oceanic forcing alone cannot explain the magnitude of the drought (Giannini et al. 2003) and in many models the spatial pattern of precipitation anomalies associated with the drought (Xue et al.). Xue et al. based on the ensemble mean of multiple GCMs participating in WAMME2 showed that SST and land cover changes are each responsible for roughly 60 and 40 % of the Sahelian precipitation changes associated with the observed drought. Based on the LUC approach in this study, for the western part of the Sahel region (Table 2), precipitation changes caused by land use change under the three different LBCs account for approximately 50–65 % of the observed drought and are equivalent

to 16–20 % of the corresponding model climatology. The RegCM in this study joins most of the WAMME2 GCMs in demonstrating that land cover changes are likely to be responsible for the unique spatial pattern of observed precipitation changes, with a strong dry signal over the Sahel region and a weak wet signal over the Guinea Coast and part of Central Africa.

Acknowledgments The research was supported by funding from the National Science Foundation (AGS-1049017, AGS-1063986, and AGS-1419526).

References

Abiodun BJ, Pal JS, Afiesimama EA, Gutowski WJ, Adedoyin A (2008) Simulation of West African monsoon using RegCM3 Part II: impacts of deforestation and desertification. Theor Appl Climatol 93(3–4):245–261

Ahmed KF, Wang GL, You LZ, Yu M (2015a) Potential impact of climate and socioeconomic changes on future agricultural land use in West Africa. Earth Syst Dyn. doi:10.5194/esdd-6-1129-2015

Ahmed KF, Wang GL, Yu M, You LZ, Koo JW (2015b) Impact of climate changes on cereal crop yields in West Africa. Clim Change. doi:10.1007/s10584-015-1462-7

Charney JG, Quirk WJ, Chow SH, Kornfield J (1977) A comparative study of the effects of albedo change on drought in semi-arid regions. J Atmos Sci 34:1366–1385

Chen M, Xie P, Janowiak JE, Arkin PA (2002) Global land precipitation: a 50-yr monthly analysis based on gauge observations. J Hydrometeorol 3:249–266

Cook KH (1999) Generation of the African easterly jet and its role in determining West African precipitation. J Clim 12:1165–1184

Cook KH, Vizy EK (2012) Impact of climate change on mid-21st century growing seasons in Africa. Clim Dyn 39:2937–2955

Druyan LM, Feng J, Cook KH, Xue Y, Fulakeza M, Hagos SM, Konare A, Moufouma-Okia W, Rowell DP, Vizy EK, Ibrah SS (2009) The WAMME regional model intercomparison study. In: Special issue "West African monsoon and its modeling". Clim Dyn 35:175–192. doi:10.1007/s00382-009-0676-7

Fan Y, van den Dool H (2008) A global monthly land surface air temperature analysis for 1948-present. J Geophys Res 113:D01103. doi:10.1029/2007JD008470

Fuller D, Ottke C (2002) Land cover, rainfall and land-surface Albedo in West Africa. Clim Change 54:181–204

Giannini A, Saravanan R, Chang P (2003) Oceanic forcing of Sahel rainfall on interannual to interdecadal time scales. Science 302:1027–1030

Giorgi F et al (2012) RegCM4: model description and preliminary tests over multiple CORDEX domains. Clim Res 52:7–29

Gornitz V (1985) A survey of anthropogenic vegetation changes in West Africa during the last century—climatic implications. Clim Change 7:285–325

Hagos S, Cook KH (2008) Ocean warming and late-twentieth century Sahel drought and recovery. J Clim 21:3797–3814

Hagos S, Leung LR, Xue YK et al (2014) Assessment of uncertainties in the response of the African monsoon precipitation to land use change simulated by a regional model. Clim Dyn 43:2765–2775. doi:10.1007/s00382-014-2092-x

Hurtt GC, Chini LP, Frolking S et al (2011) Harmonization of land-use scenarios for the period 1500–2100: 600 years of global gridded annual land-use transitions, wood harvest, and resulting secondary lands. Clim Change 109:117–161. doi:10.1007/s10584-011-0153-2

Kanamistu M, Ebisuzaki W et al (2002) NCEP-DOE AMIP-II reanalysis (R-2). Bull Am Meteorol Soc 83:1631–1643

Koster R et al (2004) Regions of strong coupling between soil moisture and precipitation. Science 305:1138–1140

Kucharski F, Zeng N, Kalnay E (2013) A further assessment of vegetation feedback on decadal Sahel rainfall variability. Clim Dyn 40(5–6):1453–1466

Lawrence PJ, Chase TN (2007) Representing a new MODIS consistent land surface in the Community Land Model (CLM 3.0). J Geophys Res 112:G01023. doi:10.1029/2006JG000168

Legates DR, Willmott CJ (1990) Mean seasonal and spatial variability in gauge corrected, global precipitation. Int J Climatol 10:111–127

Lu J, Delworth TL (2005) Oceanic forcing of the late 20th century Sahel drought. Geophys Res Lett 32:L22706. doi:10.1029/2005GL023316

Mei R, Wang GL, Gu HH (2013) Summer land-atmosphere coupling strength over the U.S.: results from a regional climate model RegCM4.0-CLM3.5. J Hydrometeorol 14:946–962. doi:10.1175/JHM-D-12-043.1

Neale RB, Chen CC, Gettelman A et al (2012) Description of the NCAR Community Atmosphere Model (CAM 5.0). Technical Note NCAR/TN-486+STR, National Center for Atmospheric Research, Boulder, Colorado, 274 pp

Oleson KW, Lawrence DM, Bonan G et al (2010) Technical description of version 4.0 of the Community Land Model (CLM). Technical Note NCAR/TN-478+STR, National Center for Atmospheric Research, Boulder, Colorado, 257 pp

Paeth H, Thamm H-P (2007) Regional modeling of future African climate north of 15°S including greenhouse warming and land degradation. Clim Change 83:401–427

Paeth et al (2009) Regional climate change in tropical Northern Africa due to greenhouse forcing and land use changes. J Clim 22:114–132

Saini R, Wang GL, Yu M, Kim JH (2015) Comparison of RCMs and GCMs projections of summer precipitation in West Africa. JGR-Atmos 120:3679–3699. doi:10.1002/2014JD022599

Steiner A, Pal JS, Rauscher S et al (2009) Land surface coupling in regional climate simulations of the West African monsoon. Clim Dyn 33(6):869–892. doi:10.1007/s00382-009-0543-6

Sylla B, Pal JS, Wang GL, Lawrence PJ (2015) Impact of land surface characterization on regional climate modeling over West Africa. Clim Dyn. doi:10.1007/s00382-015-2603-4

Taylor CM, Lambin EF, Stephenne N, Harding RJ, Essery RLH (2002) The influence of land use change on climate in the Sahel. J Clim 15:3615–3629

Vizy EK, Cook KH, Crétat J, Neupane N (2013) Projections of a wetter Sahel in the 21st century from global and regional models. J Clim 26:4664–4687

Wang GL, Eltahir EAB (2000a) Ecosystem dynamics and the Sahel drought. Geophys Res Lett 27(6):795–798

Wang GL, Eltahir EAB (2000b) The role of ecosystem dynamics in enhancing the low-frequency variability of the Sahel rainfall. Water Resour Res 36(4):1013–1021

Wang GL, Eltahir EAB, Foley JA, Pollard D, Levis S (2004) Decadal variability of rainfall in the Sahel: results from the coupled GENESIS-IBIS atmosphere-biosphere model. Clim Dyn 22(6–7):625–637. doi:10.1007/s00382-004-0411-3

Wang GL, Miao Y, Pal JS, Rui M, Bonan G, Levis S, Thornton P (2015) On the development of a coupled regional climate-vegetation model RCM-CLM-CN-DV and its validation in tropical Africa. Clim Dyn. doi:10.1007/s00382-015-2596-z

Willmott CJ, Matsuura K (1995) Smart interpolation of annually averaged air temperature in the United States. J Appl Meteorol 34:2577–2586

Xue YK, Shukla J (1993) The influence of land surface properties on Sahel climate. Part I: desertification. J Clim 6:2232–2245

Xue YK, Sellers PJ, Kinter JL III, Shukla J (1991) A simplified biosphere model for global climate studies. J Clim 4:345–364

Xue YK, Hutjes RWA, Harding RJ, Claussen M, Prince S et al (2004a) The Sahelian climate (Chapter A5). In: Kabat P, Claussen M, Dirmeyer PA, Gash JH, Deguenni LB, Meybeck M, Pielke Sr RA, Vorosmarty CJ, Hutjes RWA, Lutkemeier S (eds) Vegetation, water, humans and the climate. Springer, Berlin, pp 59–77

Xue YK, Juang H-M, Li W et al (2004b) Role of land surface processes in monsoon development: East Asia and West Africa. J Geophy Res 109:D03105. doi:10.1029/2003JD003556.PP24

Xue YK, De Sales F, Vasic R, Mechoso CR, Prince SD, Arakawa A (2010a) Global and temporal characteristics of seasonal climate/vegetation biophysical process (VBP) interactions. J Clim 23:1411–1433

Xue YK, De Sales F, Lau K-M W et al (2010b) Intercomparison and analyses of the climatology of the West African Monsoon in the West African Monsoon Modeling and Evaluation Project (WAMME) First Model Intercomparison Experiment. In: Special issue "West African monsoon and its modeling". Clim Dyn 35:3–27. doi:10.1007/s00382-010-0778-2

Xue YK, Vasic R, Janjic Z, Liu YM, Chu PC (2012) The impact of spring subsurface soil temperature anomaly in the Western U.S. on North American summer precipitation—a case study using regional climate model downscaling. J Geophys Res 117:D11103. doi:10.1029/2012JD017692

Xue YK, Jajnic Z, Dudhia J, Vasic R, De Sales F (2014) A review on regional dynamical downscaling in intra-seasonal to seasonal simulation/prediction and major factors that affect downscaling ability. Atmos Res 147–148:68–85. doi:10.1016/j.atmosres.2014.05.001

Yu M, Wang GL (2014) Impact of bias correction of lateral boundary conditions on regional climate projections in West Africa. Clim Dyn 42:2521–2538. doi:10.1007/s00382-013-1853-2

Yu M, Wang GL, Pal JS (2015) Impact of vegetation feedback on future climate change over West Africa. Clim Dyn. doi:10.1007/s00382-015-2795-7

Zeng N, Neelin JD, Lau KW, Tucker CJ (1999) Enhancement of interdecadal climate variability in the Sahel by vegetation interaction. Science 286:1537–1540

Zhan X, Xue Y, Collatz GJ (2003) An analytical approach for estimating CO_2 and heat fluxes over the Amazonian region. Ecol Model 162:97–117